Synchrotron–Tomography on Metallic Foams

A. Haibel and J. Banhart

Hahn–Meitner–Institute Berlin, Glienicker Str. 100, 14109 Berlin, Germany

Abstract

Metallic foams are a class of materials with unique properties. In contrast to most aqueous foams which are stable due to surface active agents, the liquid state of metallic foams can be stabilized by admixing small non-soluble particles. We present the results of our investigations on such materials consisting of three different components: an aluminium alloy, silicon carbide particles for foam stabilization, and titanium hydride acting as blowing agent. By means of synchrotron–tomography we visualized the three dimensional distribution of the silicon carbide and the titanium hydride particles in the unfoamed cast solid precursor, in the fully foamed liquid state, and in the solidified final state of the foam. We analyzed the silicon carbide particle formation in these three foaming stages and its influence of the pore stability.

Metallic foams are highly porous materials. In most cases they consist of aluminium or zinc alloys mixed with titanium or zirconium hydride particles as blowing agent. Due to the low density, the high specific stiffness, and the high energy absorption capability metallic foams become more and more popular for industrial applications, e.g. for light–weight constructions, for passive safety as crash absorbers in automobile construction, or for sound and vibration damping. Some examples of engineering components made of aluminium foam are shown in Figure 1.

Figure 1: Engineering components made of aluminium foam (courtesy of IFAM, Bremen).

Our research topics aim at the understanding of the physical processes during foaming and on the optimization of production by varying the manufacturing parameters. The objective is to adjust and improve the pore size distribution, the wall thickness, the density, the homogeneity, and foam stability during the foaming process.

We present our results of tomographic investigations on aluminium based foams provided by the Department of Material Science of the University of Cambridge. The cast solid precursor of this foam consists of the aluminium alloy $AlSi10Mg$ and embedded particles of the blowing agent titanium hydride (TiH_2). After heating up precursor samples to above the decomposition temperature of the blowing agent and the melting temperature of the metal, hydrogen is released in the melt and a porous structure is generated. To achieve a sufficient stability of the metallic foam during the foaming process, 10 vol.% of insoluble,

partially wetting, micrometer–sized silicon carbide particles (SiC) were added to the alloy. Due to their partial wetting SiC particles are assumed to accumulate on the pore surfaces. Furthermore, the viscosity of the melt increases during the foaming process while the surface tension decreases. This leads to a uniform pore structure. Drainage along the walls is reduced and bubble collapses are slowed down [1–5].

The aim of our investigation is to understand the mechanism of pore stabilization by these silicon carbide particles. Synchrotron–microtomography has been shown to be an appropriate measurement method for non–destructively analyzing the entire pore and particle formation and their correlation [6–8].

The measurement were carried out at the beamline "BAMline" at BESSY [6]. The well defined and adjustable, highly intensive synchrotron radiation allows for a high spatial resolution and a very good signal–to–noise ratio. Moreover, by monochromizing the beam we are able to distinguish between regions of different absorption in the samples. The X–ray energy range is tunable between 6 and 60 keV.

Because silicon carbide and the aluminium alloy have nearly the same absorption coefficient ($\mu_{SiC} = 5.7\,\mathrm{cm}^{-1}$ and $\mu_{AlSi10Mg} = 5.0\,\mathrm{cm}^{-1}$), we need this monochromatic synchrotron radiation ($E = 25\,\mathrm{keV}$, $\Delta E/E = 10^{-2}$) to separate the two materials (Fig. 2).
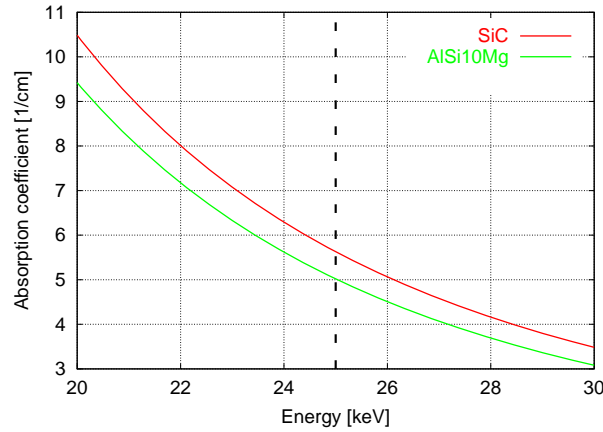

Figure 2: The X–ray absorption coefficients of silicon carbide and the aluminium alloy differ only slightly.

Figure 3 shows the tomograms of the cast solid precursor of the AlSi10Mg alloy containing 10 vol.% SiC and 0.5 vol.% TiH$_2$. The SiC particles have an average size of 70 μm. In spite of
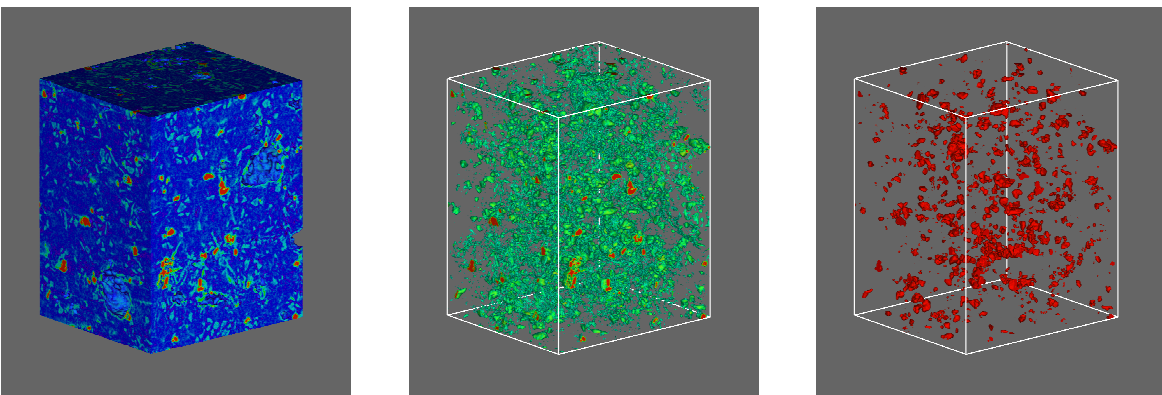

Figure 3: Cast solid precursor of AlSi10Mg with **70 μm** SiC particle size (side length: 2 mm). left: Tomogram of the metallic precursor, center: Distribution of the SiC– and TiH$_2$–particles separated from the matrix, right: Titanium hydride particle distribution alone.

2

the similar absorption coefficients, the SiC particles (cyan) are clearly distinguishable from the aluminium matrix (blue). In the second picture the alumininum matrix has been set to transparent so that the homogeneous SiC distribution becomes visible. The right figure shows only the titanium hydride particles (red) whose absorption coefficient differs markedly from that of the aluminium alloy.

The second set of tomographic pictures in Fig. 4 differs from that in Fig. 3 only by the silicon carbide particle size which is $13\,\mu$m. Both measurements were made with a spatial

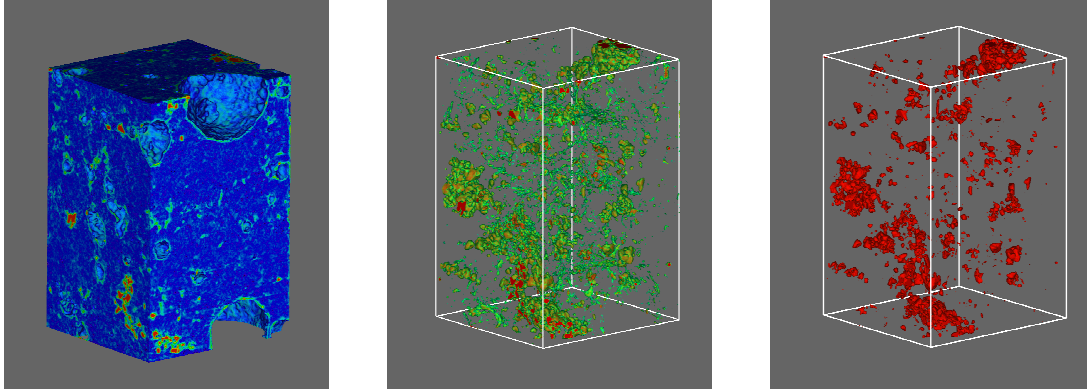Figure 4: Same as Fig. 3, but **13 μm** SiC particle size (side length: $2\,$mm).

instrument resolution of $5.4\,\mu$m.

In order to verify our results we compared the tomographic pictures with pictures obtained by two other measurement methods. Such a comparisation using a 2D–slice of a sample is shown in Figure 5. The left picture shows a tomographic slice of an aluminium alloy precursor sample with $70\,\mu$m SiC particles. The second picture represents the EDX mapping (Energy dispersed X–ray spectroscopy) of the same sample region after cutting and polishing the sample. The right picture was made using light microscopy. Comparing these slices we found the same SiC and TiH$_2$ particle formations in all three pictures, i. e. our tomographic measurements lead to reliable results. This result proves that we are able to investigate the
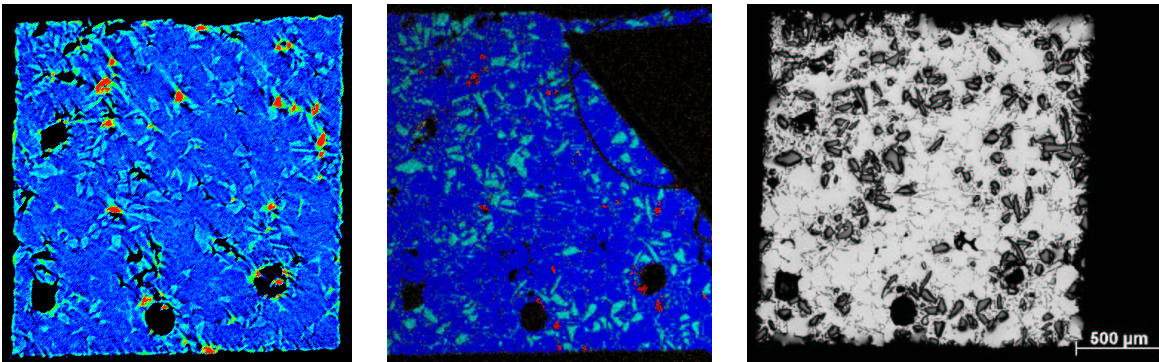

Figure 5: Left: tomographic slice of an aluminium alloy precursor with $70\,\mu$m SiC particles. The red particles are the blowing agent TiH$_2$. Center: The same sample slice obtained from a cut and polished sample by EDX (contacted in the upper right black region). Right: A light microscopical picture of the same region. (same scale in all pictures)

3D pore and SiC particle distribution by synchrotron–tomography which has the advantage of yielding an averaged information directly. At first we compared the tomograms of the unfoamed and foamed materials visually. In Figure 6 a tomographic clip of the foamed metal and the magnification of one pore wall are depicted.
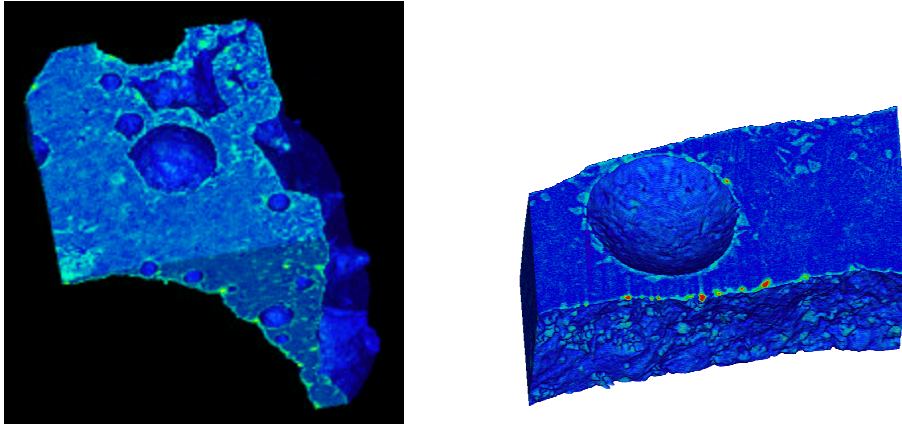
Figure 6: Left: Spatial arrangement of the silicon carbide particles in the tomogram of the foamed material (side length: 2 mm). The picture on the right side is a magnification of a single pore.

As a first visual result we see that in the unfoamed state the SiC particles are distributed quite homogeneously (Figs. 3 and 4) whereas in the foamed state the particles seem to accumulate preferentially on the pore surfaces (Fig. 6). Light microscopical pictures of sections of foamed sample slices containing $70\,\mu$m SiC particles as well as $13\,\mu$m SiC particles confirm this accumulation on the pore surfaces (see Fig. 7).
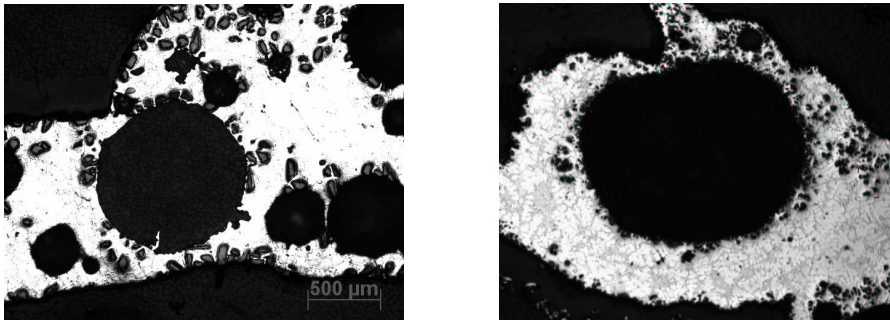

Figure 7: Two light microscopical pictures of sections of foamed samples are shown. The silicon carbide particles seem to accumulate preferentially on the pore walls; left: $70\,\mu$m particle size, right: $13\,\mu$m particle size.

For a quantitative analysis of the pore to particle correlation the information of the tomographic data must be separated into the found distinguishable components. This separation process is demonstrated in Figure 8 on a two dimensional slice. From the original data three records are created which contain only the information of the pores (left), of the SiC particles (center) and of the TiH$_2$ particles (right). For this separation all voxels within a given absorption range are chosen and assigned to the corresponding material. All these voxels get the value one, the other voxels of the record are assigned to have the value zero. The separated records of the pores and the SiC particles are needed for the correlation calculation. Due to the very similar absorption coefficients of the aluminium matrix and the SiC particles the separation of SiC is quite sensitive and difficult and the data contains a lot of noised. A so called opening algorithm is proved to be able to reduce these effects. In Figure 9 the principle is sketched.

In the first step the surfaces of all existing particles were eroded by one voxel layer. Single voxels and small voxel clusters, i. e. the noise, disappear. In the second step all the particle surfaces were dilated back by one voxel. Thus the real particle structure remains unchanged.
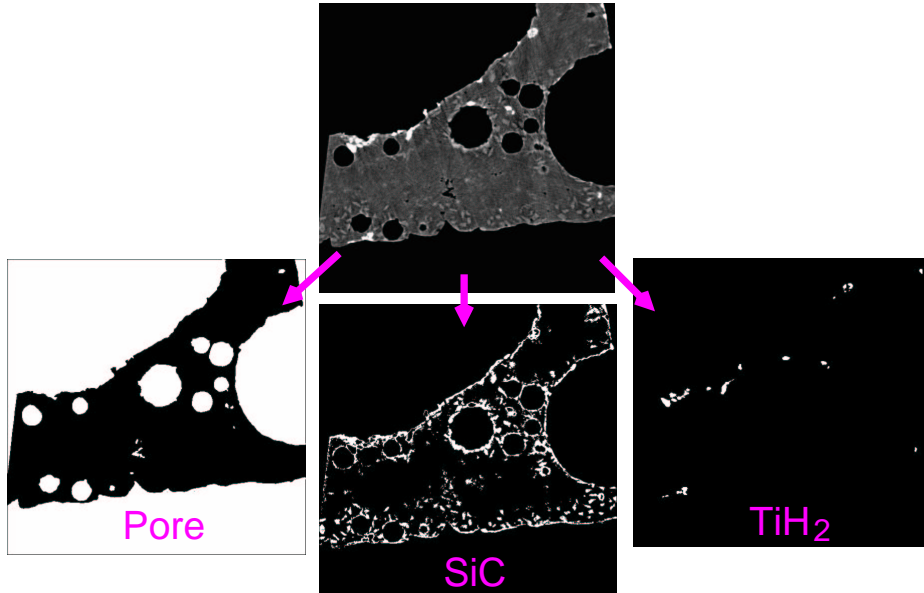
Figure 8: The original data, shown on a 2D slice of a tomogram, were separated into the different components.

The correct SiC particle separation was verified by calculating the volume fraction of all resulting particle voxels and compared to the known preparation concentration. 10 vol.% of SiC were added to the alloy. In a very good accordance with this data we found a volume fraction of 10.004 vol% for the sample containing $70\,\mu$m sized SiC particles. Caused by the spatial resolution limit of $5.4\,\mu$m it is more difficult to separate the particles for the sample with $13\,\mu$m SiC particle size. We found a volume fraction of 6.065 vol% in this case.
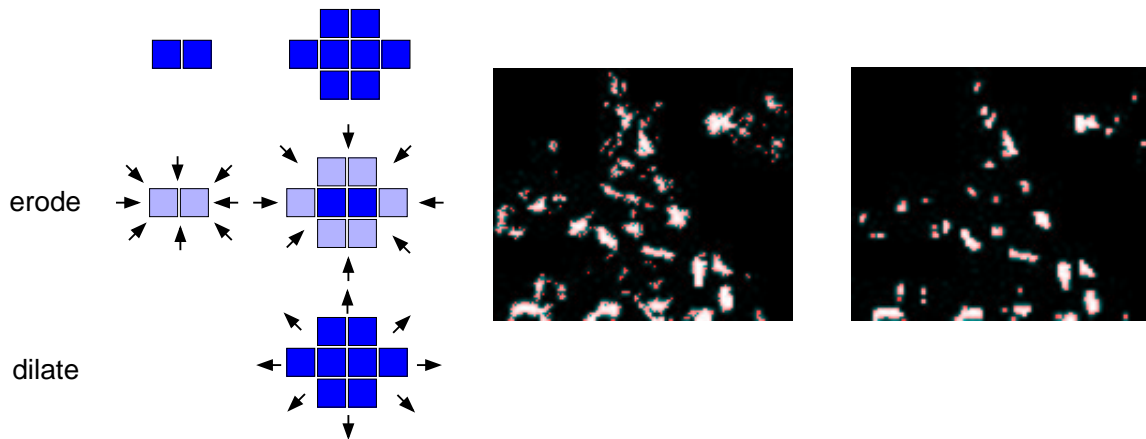

Figure 9: Left: 2D–sketch of the mathematical opening algorithm consisting of the erosion and the dilatation process to reduce noise. Center: Close-up of the original data. Right: The separated SiC particles after the opening.

In order to quantify the spatial correlation between the pores and the SiC particle positions the pores identified in a binary 3D record were sequentially dilated step by step [8]. After each of these dilatation steps the SiC particle voxels, saved in a second binary record, which became included in the increasing pore volume were counted. If this fraction of added particles decreases while dilating a correlation between pore and particle position exists. If the number of added particles is almost constant the spatial arrangement of pores and particles is independent, i.e. there are no correlations. Figure 10 represents the calculated results using this algorithm for the precursor states (left) and for the fully foamed final materials (right).
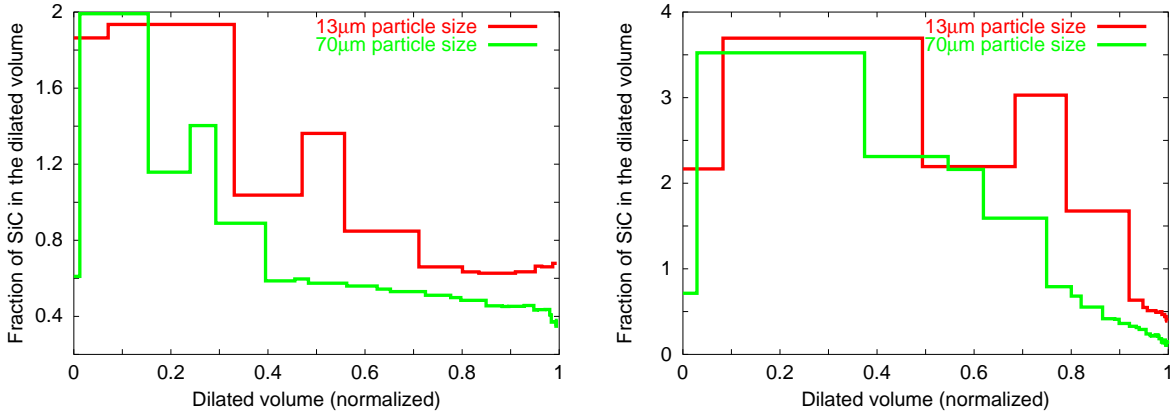
Figure 10: Correlation diagram of shortly foamed (left) and fully foamed (right) alloys.

One has to take into account that surface scattering on the pore walls (see Fig. 11) creates unrealistically high absorption coefficients leading to artefacts. Unfortunately this apparent absorption coefficient accidentally equals the absorption coefficient of the SiC. Therefore the first correlation step provides an insignificant result and has to be ignored.
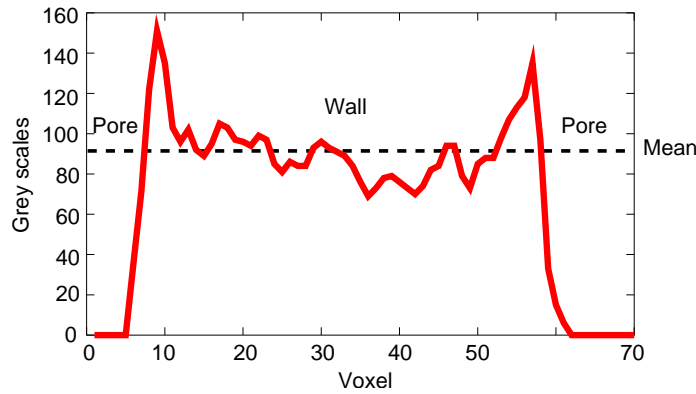

Figure 11: Cut across a pore wall. Due to scattering on the pore surfaces the average grey value of the edges on both sides of the wall, i.e. the absorption coefficient, is incorrectly increased.

In the left picture of Figure 10 the correlation calculations of the two precursor materials containing $13\,\mu m$ and $70\,\mu m$ SiC particles are plotted. During the preparation process consisting of admixing titanium hydride particles to a molten alloy, the precursor material already contains some pores although nominally unfoamed [9, 10]. Therefore, the tomography revealed the existence of the beginning of the foaming process, leading to a slight increase of SiC particles near those areas where pores were starting to grow. In these regions correlations between pores and particles can be observed. Outside this region in the bulk material no correlation exists. The number of added particles remains nearly constant.

In the right picture of Figure 10 the correlations for two foamed samples with $13\,\mu m$ as well as with $70\,\mu m$ SiC particle size are plotted. In this foaming state a correlation between the pores and the particle accumulation is obviously even far away from the cell walls.

Several arrangement mechanisms can be assumed to lead to the observed SiC particle accumulation around the pores. Due to the partial wettability of the SiC particles they should preferentially accumulate on the pore surfaces during the foaming process in the liquid state. On the other hand the particles could act as nucleation centers during foaming, the pores accrue around the SiC particles. Third the SiC particles could be pushed into the pore walls during the solidification by the proceeding solidification front.

In order to decide between these three assumed arrangement mechanisms tomographic mea-

surements were performed in the liquid foaming state. For this purpose, we used a heating set up for foaming the material during the tomographic measurements consisting of a heating lamp and a sample holder made of refractory clay (Fig. 12). For controlling the foaming temperature a thermocouple was placed directly beneath the sample.

Figure 12: Heating set up for tomography on liquid foams, consisting of a heating lamp and a sample holder made of refractory clay. A thermocouple is located directly beneath the sample.

The foaming process takes place at temperature of T=590°C and was monitored obtaining simple radiographic images every 2 seconds. The tomographic measurements were performed after the foaming process had come to an end but still in the liquid state. The measurement time amounted about 20 minutes.

As a first result of these measurements Figure 13 displays a tomographic crop of such a liquid foam containing $70\,\mu$m SiC particles. In the right picture the aluminium matrix is made transparent. Because the foam structure has to be stable during this measurements we
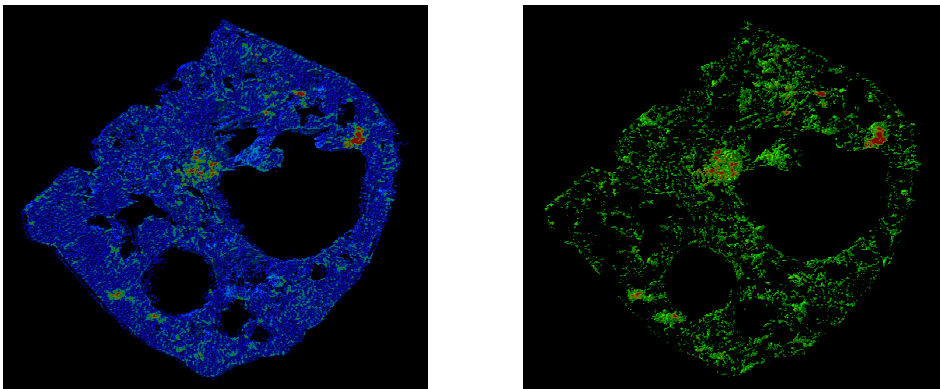

Figure 13: Tomographic crop of a liquid foam (size length: $2\,$mm). The same crop on the right shows only the SiC (green) and TiH_2 (red) particles whereas the rest of the matrix is transparently depictured.

had to wait until the foaming process completed. Therefore, the pores seen in Figure 13 in are partially collapsed. However, our first results demonstrate the feasibility of tomographic measurements of liquid metallic foams.

A correlation between the spatial arrangement of the pores and the SiC particles is hard to prove from these first results shown in Figure 13. The first correlation analysis of this data shows a weak correlation implying that the particle accumulation on the pore surfaces might take place not only in the liquid state due to partial wetting of the particles but also during solidification. However, we shall continue this project of tomography on liquid foams
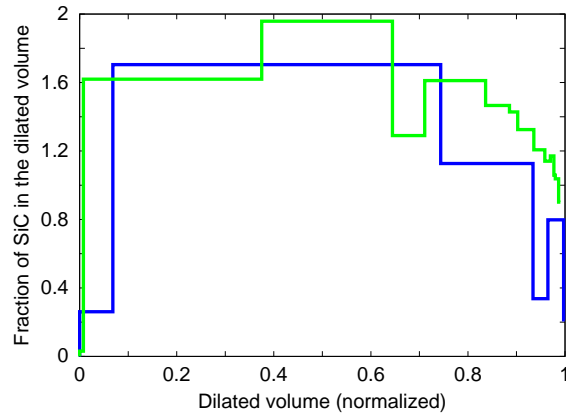
Figure 14: Results of the correlation calculation are shown for two different liquid foams with SiC particles of $70\,\mu$m diameter.

with a higher spatial resolution and shall also include samples with $13\,\mu$m SiC particle size to obtain more significant data.

References

[1] Ip, S.W., Wang, Y., and Toguri, J.M., *Aluminium Foam Stabilization by Solid Particles*, Can. Met. Quarterly, vol. 38, no. 1, 1999

[2] Prakash, O., Sang, H., Embury, J.D., *Structure and Properties of Al-SiC foams*, Materials Science and Engineering A199, 1995

[3] Kaptay, G., *Interfacial criteria for ceramic particle stabilised metallic foams*, Proceedings of MetFoam 99, Bremen, Germany, 1999, Eds. J. Banhart, M.F. Ashby, N.A. Fleck

[4] Jin, I., Kenny, L.D. and Sang, H., *Stabilized Metal Foam Body*, U.S. Patent 5 112 697, 1992

[5] Wood, J.T., *Production and Applications of Continuously Cast, Foamed Aluminium*, Proceedings of the Symposium on Metal Foams, Stanton, Delaware, 1997, Eds. J. Banhart and H. Eifert

[6] G. Weidemann, J. Goebbels, Th. Wolk, H. Riesemeier, *"First computed tomography experiments at BAMline"*, BESSY Annual Report 2001

[7] A. Haibel, A. Rack, G. Weidemann, H. Riesemeier, J. Goebbels, J. Banhart, *"Synchrotron-μ–Tomography on Aluminium and Zinc Foams"*, BESSY Annual Report 2002

[8] L. Helfen, H. Stanzick, J. Ohser, K. Schladitz, P. Pernot, J. Banhart, and T. Baumbach, *"Investigation of the Foaming Process of Metals by Synchrotron-Radiation Imaging"* Proc. of the SPIE SS/NDE conference, 2003, in press

[9] Gergely, V., Degischer H.P., and Clyne T.W., Comprehensive composite materials, vol. 3 Amsterdam Elsevier Science, 2000

[10] Gergely, V. and Clyne, T.W., *A Novel Melt–Based Route to Aluminium Foam Production*, Proceedings of the Conference on MetFoam 99, Bremen, Germany, 1999, Eds. J. Banhart, M.F. Ashby, N.A. Fleck